



Dynamic Behaviour of a Population of Controlled-by-price Demand Side Resources

Sossan, Fabrizio; Han, Xue; Bindner, Henrik W.

Published in:

Proceedings of the 2014 IEEE Power and Energy Society General Meeting.

Link to article, DOI:

[10.1109/pesgm.2014.6939320](https://doi.org/10.1109/pesgm.2014.6939320)

Publication date:

2014

Document Version

Early version, also known as pre-print

[Link back to DTU Orbit](#)

Citation (APA):

Sossan, F., Han, X., & Bindner, H. W. (2014). Dynamic Behaviour of a Population of Controlled-by-price Demand Side Resources. In Proceedings of the 2014 IEEE Power and Energy Society General Meeting. IEEE. DOI: 10.1109/pesgm.2014.6939320

General rights

Copyright and moral rights for the publications made accessible in the public portal are retained by the authors and/or other copyright owners and it is a condition of accessing publications that users recognise and abide by the legal requirements associated with these rights.

- Users may download and print one copy of any publication from the public portal for the purpose of private study or research.
- You may not further distribute the material or use it for any profit-making activity or commercial gain
- You may freely distribute the URL identifying the publication in the public portal

If you believe that this document breaches copyright please contact us providing details, and we will remove access to the work immediately and investigate your claim.

Dynamic Behaviour of a Population of Controlled-by-price Demand Side Resources

Fabrizio Sossan, Xue Han and Henrik Bindner
Center for Electric Power and Energy, DTU Elektro
Technical University of Denmark
Roskilde, Denmark
{faso, xueh, hwbi}@elektro.dtu.dk

Abstract—It is described that controlling or shedding by price the power consumption of a population of thermostatic loads introduces in the aggregate consumption dynamic effects that cannot be disregarded if electrical flexible demand is meant to supply power system services. It is shown that inducing a desynchronization in the consumption contributes to damp the oscillations. Results are supported by Monte Carlo simulations of a population of buildings equipped with electric space heating whose consumption is indirect controlled by a dynamic price of the electricity.

I. INTRODUCTION

The increasing cost of traditional sources for electricity generation and the thrust towards a more sustainable impact of human activities on planet Earth are leading the need of integrating more renewable energy in the power system. The axiom on which the power system is based is that the electric generation has to match the consumption and this is accomplished by regulating the production to respond to system frequency variation. Increasing the share of generation from renewable sources decreases the amount of controllable production in the grid limiting the penetration that renewables can achieve.

A solution that is envisaged for restoring the lack of controllability is controlling the electric power demand. Such a solution is dated back in time [1]. However it has been revitalized in the recent years because the promising transition to smart grid constitutes an adequate enabling technology for realizing it in large scale and in an automated way. Control-by-price or indirect control is often mentioned as a way for supplying regulating power and supporting the ancillary services of the electric grid. The need of regulating power of the grid is reflected into a dynamic energy price that is used for inducing a shift (or sometimes a shedding) in the power consumption of demand side resources (DSRs). DSRs are electric loads whose consumption can be shifted without impacting the quality of the primary services they are supplying to the consumers. The paradigm of controlling flexible demand is that the contribution in terms of electric power support from the single DSR is not relevant for the power system while the aggregate and coordinate contribution from a large population of DSRs might have important size and hence the capability of impacting the operation of the electric grid. Nevertheless flexible consumption cannot be regarded as a fully controllable virtual unit as the aggregate electric power consumption primarily depends on consumers demand and DSRs operational constraints.

Load kickback effect, are investigated originally under the circumstances of restoration from a power system outage [2]. It is due to the fact that the usual diversity of different loads is lost and they have temporary synchronized behaviour. Under the smart grid frame, the kickback effect may happen as well: the ancillary services instruct the DSRs to perform same or similar actions to their flexible consumption. [3] presented the load kickback model of water heaters. The kickback curve is formulated as a function of curtailed energy using regression method. In [4], the software EnergyPlus is used to identify the payback effects of the components inside the building (e.g., space-heating and air-conditioning systems) by specifying the thermostat model. The kickback effects are observed from a large population of thermostat loads in some studies [5] and a control strategy for reducing it is proposed in [6]. However, given the increasing importance of demand response in the power system, the dynamic behavior of the aggregate demand should be investigated specifically.

In this paper, the dynamic behavior of the aggregate response of an indirect controlled population of DSRs is studied. A sensitivity analysis through Montecarlo simulations is performed considering a homogeneous (i.e. same kind of DSR but not same characteristics) population of 100×10^3 thermostatic controlled loads (building electric space heating) and it is shown how controlling them with an identical indirect control signal (e.g. price signal) introduces time dynamic effects that need to be taken into account if flexible demand is meant to supply regulating power to the grid or other power system services. It is also shown that inducing a diversification in the state of DSRs provide to desynchronize the aggregate consumption hence leading to a more desirable behavior for the power system. This conclusion can be considered for developing price responsive controller for indirect control capable of producing better behaving aggregate power consumption.

The paper is organized as follows: Section II describes the indirect control setup, building thermal models, price responsive control algorithm along with the description of the Monte Carlo simulations scenario. In Section III a detailed description of the kickback effect is provided and supported by simulation results. Monte Carlo simulations of the population are provided and discussed in Section IV. Conclusions are stated in Section V.

II. INDIRECT CONTROL SETUP

The indirect control setup that is considered for supplying power system services is the one shown in Fig. 1. An indirect

control signal, say the electricity price $p(t)$ (however no market considerations are given in the sequel), is used for inducing a shift in power consumption of a population of DSRs.

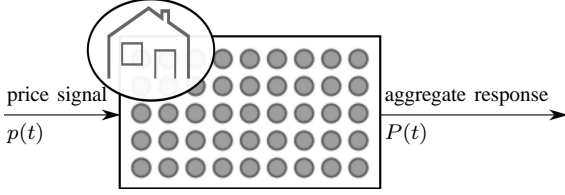


Fig. 1. Indirect control setup. A price signal indirect controls a population of 10^5 buildings equipped with electric space heating.

The population is composed by 10^5 buildings equipped with electric space heating. The aggregate power consumption $P(t)$ of the population is simulated with a bottom-up approach and combining together the individual power requirement of all buildings. Each building is described by a first order dynamic model and it is discussed in Section II-A. Each space heating unit is equipped with an price responsive control algorithm that is discussed in Section II-B. The simulations are performed using a Monte Carlo approach, i.e. buildings and control algorithms have identical form across the population but their parameters are variated according statistical distributions (Section II-C).

A. Building thermal model

The temperature T_j of each building j of the population is simulated with the first order thermal model given in Eq. 1 where input quantities ϕ_s , T^{out} are time series for solar irradiance [Wm^{-2}] and outside temperature [$^{\circ}\text{C}$] respectively and $u_j(t)$ is the controllable input (on/off) and the parameter D_j is the nominal power consumption of the space heating. The parameters C_j , R , A_j are respectively the lumped thermal capacity of the building, the thermal resistance of the building towards the exterior environment and the window area. C_j and A_j are parameters depending on the size of the building and the criteria with which they have been assigned is explained in the sequel. $\eta_j(t)$ in Eq. 1 is a zero mean Gaussian noise term which is introduced for further differentiating the behavior of the models in the Monte Carlo simulations.

$$C_j \frac{dT_j(t)}{dt} = -\frac{1}{R} T_j(t) + D_j u_j(t) + A_j \phi_s(t) + \frac{1}{R} T^{out}(t) + \eta_j(t) \quad (1)$$

The parameters of the thermal model in Eq. 1 of Power Flexhouse are reported in Table I. Power Flexhouse is a free standing building and it is used as facility for testing demand side management strategies at DTU Elektro, Denmark [7].

TABLE I. POWER FLEXHOUSE I ORDER THERMAL MODEL PARAMETERS.

| Name | Unit | Value |
|----------|-------------------------------|--------------------|
| C_{FH} | [kW $^{\circ}\text{C}^{-1}$] | 12.3×10^3 |
| S_{FH} | [m^2] | 125 |
| A_{FH} | [m^2] | 10.7 |

The values of the parameters in Table I (which are obtained by grey-box modelling) are used as base values for deriving

those of all the other models in the population. While the value of the thermal resistance R is kept constant across the population (it is assumed that the buildings have same insulation characteristic), the values C_j and A_j are respectively obtained using the expressions in Eq. 2 and Eq. 3 where S_j is the size [m^2] of the building j and S_{FH} is the one of Power Flexhouse.

$$C_j = \frac{S_j}{S_{FH}} C_{FH} \quad (2)$$

$$A_j = \sqrt{\frac{S_j}{S_{FH}}} A_{FH} \quad (3)$$

In other words each C_j and A_j are scaled according the size of the building they represent (an explanation of the empirical relationships in Eq. 2 and Eq. 3 is provided later). The size S_j [m^2] of each building is a Gamma distributed random variable and it is given in Eq. 4. The histogram of 100×10^3 realizations from Eq. 4 is shown in Fig. 2. The distribution in Eq. 4 and the associated parameters k, θ have been obtained performing a statistical analysis of the size of the class of buildings whose Power Flexhouse is representative using data from the Danish National Register of Buildings (BBR) [8].

$$S_j \sim \Gamma(k, \theta) \quad \text{with } k = 22.35 \vee \theta = 1/6.71 \quad (4)$$

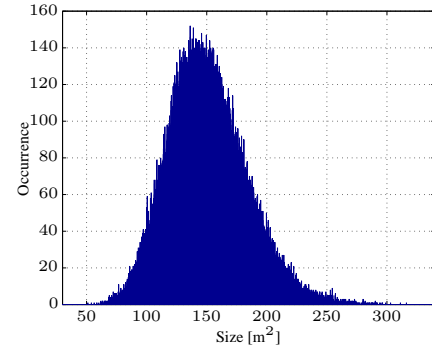


Fig. 2. Stochastic realizations from the Gamma distribution in Eq. 4.

The motivations for Eq. 2 and Eq. 3 are hereafter explained. The thermal capacity of building is due both to its air content and envelope thermal mass. Assuming constant building height, the air volume is linear with the building size S_j . Assuming rectangular shape and same sides ratio of the buildings, the lateral surface of the building is proportional to the square root of building size S_j . Assuming constant thermal resistance, the thickness of the insulation layer ($R \propto$ thermal conductor thickness on exchange area) has to grow linearly with the lateral surface hence linearly with the square root of the building size S_j . As the volume of the insulation layer and walls is given by the lateral surface times the envelope thickness (and both are linear with the square root of the building size) it can be concluded that the volume of the building envelope is also linear with S_j . In case of parameter A_j , it is assumed that the window area of each building j is proportional to the building lateral surface hence to the square root of the building size S_j and it is given in Eq. 3. A is the estimated value of Power Flexhouse window area and it is given in Table I.

B. Price responsive building temperature controller

Each building j of the population is equipped with a price responsive controller that acts on the top of a thermostat (feedback controller with hysteresis) as shown in Fig. 3.

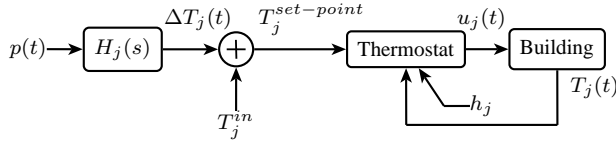


Fig. 3. Price responsive local controller + house thermostatic controller.

The price signal is elaborated by the high pass filter $H_j(s)$ whose expression is given in Eq. 5, where a_j is the temperature variation induced by an unitary stepwise change of $p(t)$ and τ_j is the filter time constant (s is the Laplace operator).

$$H_j(s) = \frac{\Delta T_j(s)}{p(s)} = \frac{a_j s}{s + \tau_j} \quad (5)$$

The steady state contribution of $H_j(s)$ is null, meaning that if the price signal does not change for sufficient long time, the original set-point is restored. This is because it is assumed that the consumers are not willing to affect their temperature comfort at steady state (nondisruptive load control).

The set-point of the thermostat $T_j^{set-point}(t)$ is given in Eq. 6 where T_j^{in} is the user indoor comfort temperature.

$$T_j^{set-point}(t) = T_j^{in} + \Delta T_j(t) \quad (6)$$

The quantity h_j in the thermostat block of Fig. 3 is the hysteresis of the controller and $u_j(t)$ represents the state of the space heating.

C. Parameters variations in the Monte Carlo simulations

Monte Carlo simulations, i.e. accounting for stochastic variations of the parameters, are performed for considering differences of both building and price responsive controller characteristics across the population. Table II shows the PDF according to which the parameters are picked and the correlation coefficients between them. Correlation among S_j (hence thermal capacity C_j) and both D_j and τ_j is introduced because the space heating nominal power and the time constant of the filter are assumed to related to the size of the building.

TABLE II. PARAMETERS DISTRIBUTIONS AND CORRELATION COEFFICIENTS ASSUMED FOR MATRIX FOR MONTE CARLO SIMULATIONS

| | PDF | C_j | A | ϕ_h | T_j | h_j | a_j | τ_j |
|------------|---|-------|-----|----------|-------|-------|-------|----------|
| C_j | $\Gamma(22,663)$ | 1 | .99 | .99 | 0 | 0 | 0 | .85 |
| A | $\Gamma(88,.13)$ | .99 | 1 | .99 | 0 | 0 | 0 | .84 |
| D_j | $80 \cdot S_j + \mathcal{N}(.25^2, 1)$ | .99 | .99 | 1 | 0 | 0 | 0 | .84 |
| T_j^{in} | $\mathcal{N}(21, .15^2)$ | 0 | 0 | 0 | 1 | 0 | 0 | 0 |
| h_j | $\mathcal{N}(1, .10^2)$ | 0 | 0 | 0 | 0 | 1 | 0 | 0 |
| a_j | $\mathcal{N}(-1.5, .1^2)$ | 0 | 0 | 0 | 0 | 0 | 1 | 0 |
| τ_j | $\frac{(S_j - 150)}{1} + \mathcal{N}(7e3, 1)$ | .85 | .84 | .84 | 0 | 0 | 0 | 1 |

III. DESCRIPTION OF THE KICKBACK EFFECT

The simulation in support of this discussion is obtained with the setup in Section II-C with the exception that the threshold of the thermostats and the parameters of the controllers are constant across the population. This is for facilitating the visualization and the description of the dynamics phenomena associated to the aggregate consumption. Solar radiation and ambient temperature (needed by thermal models) have been arbitrarily set to 0 and 10 °C respectively and they are assumed constant both in time and across the population.

The aggregate power consumption response of the buildings (Fig. 4-I) to a step variation of the price signal (Fig. 4-II) is analyzed in this section. Four points of interest have been identified along the consumption profile of Fig. 4-I and they are indicated by the colored marks. In the sequel, the instants of time that corresponds to the marks are analyzed. Fig. 4-III shows the temperature deviation that the indirect control algorithm (Section II-B) applies to each building.

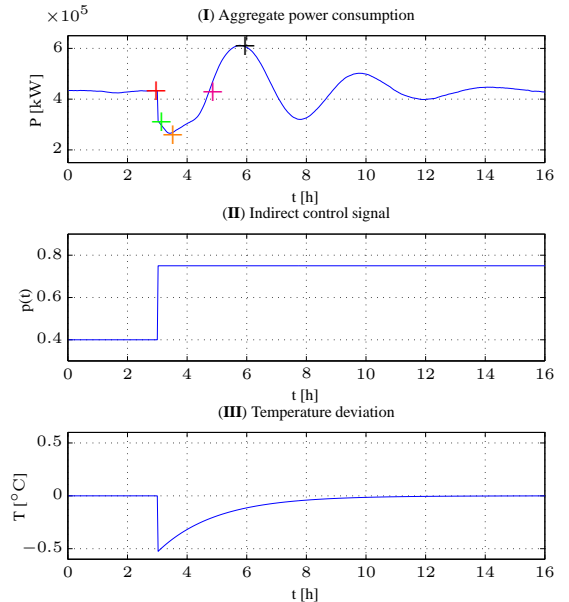


Fig. 4. Population power consumption (I) when controlled by price signal in (II). The temperature deviation produced by the algorithms is shown in (III).

Red mark (steady state): the aggregate power consumption does not exhibit any variation. This is a steady state situation and, statistically, for each thermostat turning on, there is one turning off and vice-versa. The histogram in Fig. 5 shows that the distribution of the distance between the temperature of each building and the respective set-point (i.e. $T_j(t) - T_j^{set-point}$) is uniform across the population. The buildings moving rightward are those whose space heating is *on* and those which eventually pass the right threshold are the ones switching off. The units moving leftward are cooling down (space heating off) and those which pass the left threshold are the ones switching on, hence contributing positively to the aggregate power consumption. The red bars in the histogram of Eq. 7 shows the distribution of the units state.

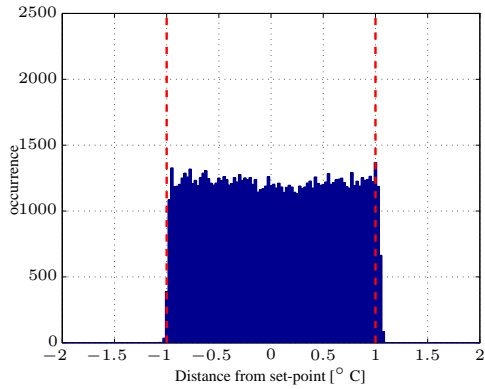


Fig. 5. Histogram of the distance of the temperature of each building from the respective set-point ($T_j(t) - T_j^{set-point}$) at the red mark of Fig. 4-I.

Green mark: the price signal variation is perceived by the indirect control algorithms which therefore decrease the temperature set-point of the respective building. All the units that are in *on* state and whose temperature is higher than the new thermostat set-point are switched off. This provokes a drop in the power consumption. By comparing Fig. 5 and Fig. 6, it is possible to notice that the histogram is shifted on the right of the thermostatic interval (whose thresholds are denoted by the two red dotted lines). A consequence of this is that – for a certain period of time – no units will be able to trigger the consumption on because they need to cool down in order to reach the new left thermostatic bound. This unbalance causes the aggregate power consumption to decrease further as shown by the power profile behavior between the green and orange marks in Fig. 4-I. The blue bars in the histogram in Fig. 7 show the distribution of the state of the space heating units for the instant of time under consideration and, as expected, the group of units in the *off* state for the instant in analysis is larger than in the steady state.

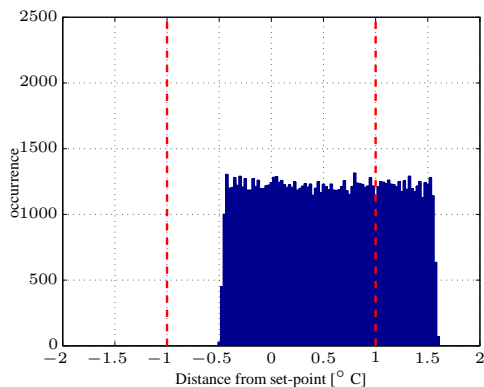


Fig. 6. Temperatures distances distribution at the green mark in Fig. 4-I.

Orange mark: the power consumption profile reaches the minimum value. The histogram in Fig. 8 shows a large number of units being in the proximity of the left thermostatic threshold and hence close to trigger the consumption on (if off). It is worth to note that while time passes, the indirect control algorithm gradually removes the temperature offset (Fig. 4-III) hence ‘accelerating’ the movement of the population in the histogram towards the center.

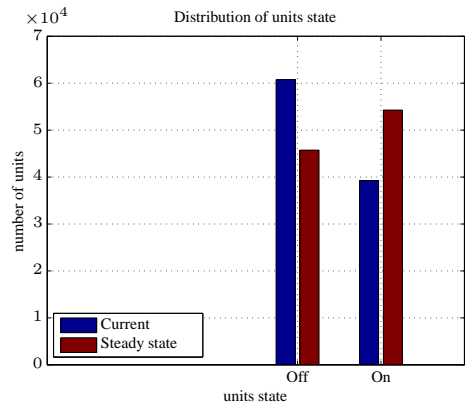


Fig. 7. Distribution of the units state across the population at steady state in the proximity of instant of time indicated with the green mark in Fig. 4-I.

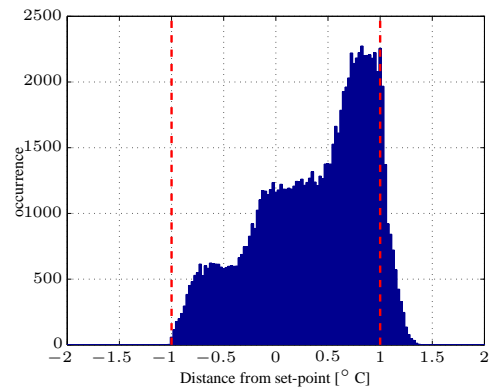


Fig. 8. Temperatures distances distribution at the orange mark in Fig. 4-I.

Magenta mark: here the aggregate power consumption assumes the same value as at steady state (red mark). However this situation does not result in an equilibrium point because the flow of units trespassing the right thermostatic threshold does not equal the flow in the opposite side. By comparing the histograms in Fig. 8 and Fig. 9 it is possible to notice that there is a ‘wave’ moving leftwards, hence composed by units that are cooling down. This unbalance will cause the aggregate power consumption to increase because a large number of units is expected to trigger the consumption on in the near future. This will cause more units to consume power concurrently and hence provoking a *kickback* effect on the aggregate power consumption (black mark).

Black mark: it corresponds to the peak of the kickback effect of the aggregate response. After the black mark, the aggregate power consumption in Fig. 4-I undergoes to a period with damped oscillations before reaching a new steady state at time $t \approx 15$ h. The steady state power consumption does not differ than the initial one because the indirect control algorithm does not introduce any steady state contribution for not altering the user comfort.

IV. MONTE CARLO SIMULATIONS

Simulations are performed with the setup discussed in Section II-C, therefore accounting for variations across the population of buildings characteristics, parameters of price responsive controller and parameters of the thermostat. Fig. 10 shows the aggregate power consumption behavior to a step

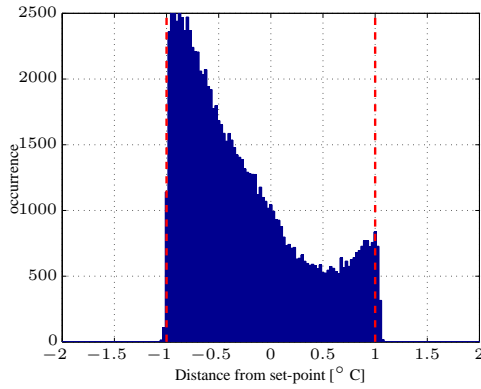


Fig. 9. Temperatures distances distribution at the magenta mark in Fig. 4-I.

variation of the price signal for three different values of the standard deviation of η ¹ (the noise term in Eq. 1) and it resembles the response of a second order system at different damping ratios. Initially, the variation of the price signal provokes a synchronization of the state of those units that switch off. A small variance noise term does not promote a diversification of the consumption for those units have been switched off that hence tend to trigger the consumption together for long time causing undamped oscillations. A large variance reduces the deep of the initial power contribution but it contributes to restore a diversification in the consumption hence the peak of the kickback effect is reduced in amplitude and spread in time. Such a characteristic is surely more desirable for the power system point of view. However the noise term is not a controllable parameters and according indirect control paradigm, a desynchronization cannot be induced by price as the signal for indirect control is the same for all DSRs.

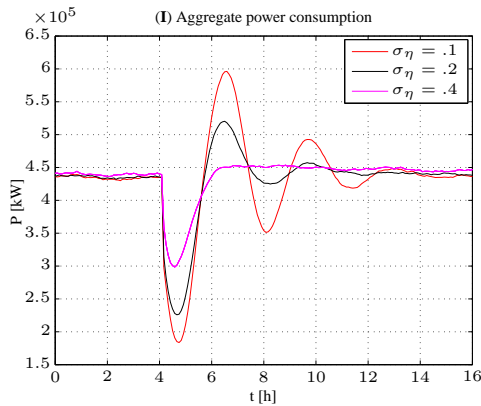


Fig. 10. Population power consumption for three values of the variance of the Gaussian noise term η in Eq. 1.

One might wonder if dynamic effects are reduced by shedding the consumption instead of shifting it. Fig. 11-I shows the aggregate power consumption of the same population discussed above with the difference that the temperature offset is not high pass filtered (Fig. 11-III). Oscillations are still present because the initial drop of power provoked by the

variation of the price signal does not match the power variation at steady state.

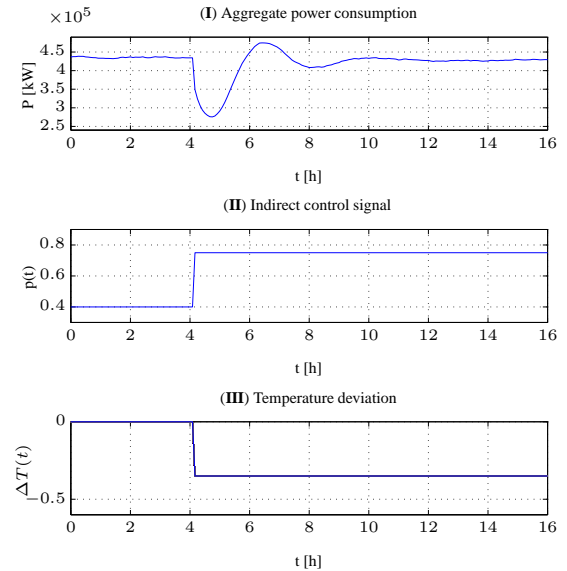


Fig. 11. Consumption shedding instead of shifting.

V. CONCLUSIONS

The topic of indirect controlling a large population of DSRs is addressed. It is shown that a variation of the price signal provokes a synchronization in the consumption of the DSRs that can lead to unwanted oscillations of the aggregate power response. The same phenomena is observed to happen also when the consumption is curtailed rather than shifted. It is shown that diversifying the state of DSRs composing the population reduce the peak of the kickback effect. This suggests that a random component could be taken into account in the local price responsive controller in order to dump the oscillations and avoid a deep a kickback.

REFERENCES

- [1] C. Gellings, "The concept of demand-side management for electric utilities," *Proceedings of the IEEE*, vol. 73, no. 10, pp. 1468–1470, 1985.
- [2] D. Miller and T. Sleva, "Cold load pickup issues," tech. rep., Power System Relay Committee of The IEEE Power Engineering Society, May 2008.
- [3] S. Lee and C. Wilkins, "A practical approach to appliance load control analysis: a water heater case study," *power apparatus and systems, ieee transactions on*, no. 4, pp. 1007–1013, 1983.
- [4] N. Ruiz, I. Cobelo, and J. Oyarzabal, "A direct load control model for virtual power plant management," *Power Systems, IEEE Transactions on*, vol. 24, no. 2, pp. 959–966, 2009.
- [5] C. Perfumo, E. Kofman, J. H. Braslavsky, and J. K. Ward, "Load management: Model-based control of aggregate power for populations of thermostatically controlled loads," *Energy Conversion and Management*, vol. 55, pp. 36–48, 2012.
- [6] N. A. Simitsyn, S. Kundu, and S. Backhaus, "Safe protocols for generating power pulses with heterogeneous populations of thermostatically controlled loads," *Energy Conversion and Management*, vol. 67, pp. 297–308, 2013.
- [7] DTU, "Powerflexhouse," 2013.
- [8] "Byggnings-og boligregistret." www.bbr.dk.

¹Standard deviations in Fig. 10 refer to the discretized thermal model (sampling time 300 s). For example, $\sigma_\eta = .1$ means that in five minutes the evolution of the model could be perturbed up to $\pm 0.2^\circ\text{C}$ at 95% of probability.